Published September 12, 2016

Epstein-Barr viral miRNAs inhibit antiviral CD4$^+$ T cell responses targeting IL-12 and peptide processing

Takanobu Tagawa,[1,2]* Manuel Albanese,[1,2]* Mickaël Bouvet,[1,2] Andreas Moosmann,[1,2] Josef Mautner,[1,2,3] Vigo Heissmeyer,[4,5] Christina Zielinski,[6] Dominik Lutter,[7] Jonathan Hoser,[8] Maximilian Hastreiter,[8] Mitch Hayes,[9] Bill Sugden,[9] and Wolfgang Hammerschmidt[1,2]

[1]Research Unit Gene Vectors, Helmholtz Zentrum München, German Research Center for Environmental Health and [2]German Centre for Infection Research (DZIF), Partner site Munich, Germany, D-81377 Munich, Germany
[3]Children's Hospital, Technical University Munich, D-80337 Munich, Germany
[4]Research Unit Molecular Immune Regulation, Institute of Molecular Immunology, Helmholtz Zentrum München, German Research Center for Environmental Health Munich and [5]Institute for Immunology, University of Munich, D-80539 Munich, Germany
[6]Institute for Medical Microbiology, Immunology and Hygiene, Technical University Munich, D-80337 Munich, Germany
[7]Institute for Diabetes and Obesity, Helmholtz Zentrum München and [8]Institute of Bioinformatics and System Biology, Helmholtz Zentrum München, German Research Center for Environmental Health, D-85764 Munich, Germany
[9]McArdle Laboratory for Cancer Research, University of Wisconsin-Madison, Madison, WI 53706

Epstein-Barr virus (EBV) is a tumor virus that establishes lifelong infection in most of humanity, despite eliciting strong and stable virus-specific immune responses. EBV encodes at least 44 miRNAs, most of them with unknown function. Here, we show that multiple EBV miRNAs modulate immune recognition of recently infected primary B cells, EBV's natural target cells. EBV miRNAs collectively and specifically suppress release of proinflammatory cytokines such as IL-12, repress differentiation of naive CD4$^+$ T cells to Th1 cells, interfere with peptide processing and presentation on HLA class II, and thus reduce activation of cytotoxic EBV-specific CD4$^+$ effector T cells and killing of infected B cells. Our findings identify a previously unknown viral strategy of immune evasion. By rapidly expressing multiple miRNAs, which are themselves nonimmunogenic, EBV counteracts recognition by CD4$^+$ T cells and establishes a program of reduced immunogenicity in recently infected B cells, allowing the virus to express viral proteins required for establishment of life-long infection.

INTRODUCTION

EBV is both ubiquitous and immunogenic. This oncogenic herpesvirus (IARC Working Group on the Evaluation of Carcinogenic Risks to Humans, 2010) has evolved multiple genes to fend off immune responses when its infection is established (Hislop et al., 2002; Rowe et al., 2007; Ressing et al., 2008; Zuo et al., 2009; Qiu et al., 2011; Rancan et al., 2015). Despite these measures, EBV-specific T cells constitute a considerable fraction of the memory T cell repertoire of the latently infected human host (Hislop et al., 2002) and are essential in controlling latent EBV infection (Moosmann et al., 2010). In fact, immunocompromised patients have an increased incidence of EBV-associated malignancies (Gottschalk et al., 2005).

EBV infects nondividing B lymphocytes, activates them, and drives them to proliferate, thus amplifying the load of viral genomes. Once activated, infected B cells acquire properties of antigen-presenting cells. After infection, they rapidly present epitopes of structural proteins from incoming virus particles and transiently express lytic genes that are otherwise characteristic of EBV's productive cycle (Kalla and Hammerschmidt, 2012). This prelatent phase of infection includes expression of two genes coding for viral immunoevasins, BNLF2a and BCRF1 (Jochum et al., 2012), which inhibit the recognition of the infected cells by EBV-specific effector T cells and natural killer cells, respectively. These two viral proteins are insufficient, however, to overcome T cell recognition (Jochum et al., 2012). Within 7–10 d, EBV establishes a latent infection in the infected B cells and expresses only few or no viral genes, which reduces their risk of becoming eliminated by the immune-competent host.

Thus, early infection could be EBV's Achilles heel, a window when the infected cell expresses and presents many viral antigens to immune cells but is inadequately protected from the host's immune response. We have now established that EBV's miRNAs overcome this vulnerability; they protect newly infected B lymphocytes from immune eradication by CD4$^+$ T cells, supporting EBV's lifelong success.

EBV encodes at least 44 microRNAs (miRNAs; Barth et al., 2011), which are small RNA regulatory molecules of ∼22 nt in length (Bartel, 2004). miRNAs encoded by herpesviruses

*T. Tagawa and M. Albanese contributed equally to this paper.

Correspondence to Wolfgang Hammerschmidt: hammerschmidt@helmholtz-muenchen.de

Abbreviations used: CTSB, cathepsin B; LCL, lymphoblastoid cell line; LMP, latent membrane protein; miRNA, microRNA; RISC, RNA-induced silencing complex.

© 2016 Tagawa et al. This article is distributed under the terms of an Attribution–Noncommercial–Share Alike–No Mirror Sites license for the first six months after the publication date (see http://www.rupress.org/terms). After six months it is available under a Creative Commons License (Attribution–Noncommercial–Share Alike 3.0 Unported license, as described at http://creativecommons.org/licenses/by-nc-sa/3.0/).

The Rockefeller University Press $30.00
J. Exp. Med. 2016 Vol. 213 No. 10 2065–2080
www.jem.org/cgi/doi/10.1084/jem.20160248

Supplemental Material can be found at:
/content/suppl/2016/09/09/jem.20160248.DC1.html

The Journal of Experimental Medicine

Downloaded from on September 29, 2016

Published September 12, 2016

are reported to play important roles in cell proliferation, development, immune regulation, and apoptosis in infected cells (Skalsky and Cullen, 2010). The EBV-encoded miRNAs have been found to control expression of several cellular genes with antiapoptotic functions, but they also reportedly down-regulate *MICB* (Nachmani et al., 2009), *CXCL11* (Xia et al., 2008), and *NLRP3* (Haneklaus et al., 2012) and thus interfere with innate immune responses and inflammation. Interestingly, *MICB*, a gene encoding a ligand for the activating receptor NKG2D expressed on T and NK cells, is also targeted by miRNAs of Kaposi sarcoma–associated herpesvirus and human cytomegalovirus (Nachmani et al., 2009; Grundhoff and Sullivan, 2011). These studies imply that certain miRNAs encoded by herpesviruses target pathways involved in innate immune recognition.

EBV's miRNAs have been studied by several groups with established, EBV-infected cell lines obtained from biopsies of nasopharyngeal carcinoma and Burkitt's lymphoma, or lymphoblastoid cell lines (LCLs) derived from infecting primary B lymphocytes with EBV in vitro (Dölken et al., 2010; Gottwein et al., 2011; Kuzembayeva et al., 2012; Riley et al., 2012; Erhard et al., 2013). High-throughput target screens using immunoprecipitation of the RNA-induced silencing complex (RISC) and deep sequencing have identified many potential targets of EBV miRNAs, but the catalogs of predicted targets assembled by different groups have a surprisingly small overlap (Klinke et al., 2014). This lack of consensus may be due to the accumulation of profound differences in gene expression between different long-term, cultivated EBV-infected cell lines that do not reflect the impact of EBV's miRNAs in vivo.

To circumvent these problems, we developed an experimental approach using primary human B lymphocytes, and analyzed them during their initial days of EBV infection (Seto et al., 2010; Vereide et al., 2014). We infected the B lymphocytes with two EBV strains with and without miRNA genes, compared the gene expression in the infected cells, and examined them for their immune recognition.

We found that EBV-encoded miRNAs regulated several immune pathways, which affected $CD4^+$ T cell differentiation and activation. In addition, key molecules important for interactions with $CD4^+$ T cells were down-regulated. EBV miRNAs repressed the secretion of IL-12, which resulted in suppression of type 1 helper T cell (Th1) differentiation. Viral miRNAs controlled gene expression of HLA class II and three lysosomal enzymes important for proteolysis and epitope presentation to $CD4^+$ T cells. Such a wholesale inhibition of adaptive immune responses by multiple miRNAs of a single pathogen is unprecedented. Our findings explain the abundance of miRNAs in complex persisting viruses, and clarify how EBV can escape elimination for the lifetime of its host in spite of intense adaptive immune responses.

RESULTS

EBV miRNAs control immune regulatory pathways

We searched for cellular targets of EBV's miRNAs, using an experimental system that closely mimics human infection in vivo. Two strains of EBV, a laboratory strain (wt/B95-8) that expresses 13 miRNAs, and its derivative (ΔmiR) that expresses none (Seto et al., 2010) were used to infect freshly isolated B lymphocytes from six donors. We used carefully titrated virus stocks and infected the cells with optimal doses of both viruses (Steinbrück et al., 2015). No differences in the percentage of infected cells were seen when comparing cells infected with wt/B95-8 versus ΔmiR EBV. RNAs were isolated on day 5 after infection and sequenced (available from GEO under accession no. GSE75776; see Materials and methods). Genes that were differentially expressed in cells infected with wt/B95-8 versus ΔmiR EBV were identified with those having an absolute z-score >1.6 (Fig. 1 A and Table S1). These genes included the published miRNA targets *LY75/DEC205* (Skalsky et al., 2012) and *IPO7* (Dölken et al., 2010). Genes that were consistently down-regulated in wt/B95-8 EBV-infected cells were grouped according to the Kyoto Encyclopedia of Genes and Genomes (KEGG) pathway categories (Fig. 1 B). Down-regulated genes were predominant in pathways linked to apoptosis, cell cycle regulation, and p53 signaling, which were previously proposed to be regulated by EBV miRNAs (Seto et al., 2010; Feederle et al., 2011a,b; Vereide et al., 2014). Unexpectedly, EBV's miRNAs also regulated a wide array of genes with functions in immunity, such as cytokine–cytokine receptor interactions, antigen processing, and HLAs and co-stimulatory molecules (Fig. 1, B and C; and Table S1). We immunoprecipitated RISC (RISC-IP) and found that 14.5% (±2.4% SD) of all miRNAs were of viral origin in wt/B95-8 EBV-infected cells, dominated by miRNAs of the BHRF1 gene cluster (Fig. 1 D). No appreciable viral miRNA reads were found in cells infected with ΔmiR EBV (Fig. 1 D), suggesting that the B lymphocytes of six donors were free of EBV field strains. In wt/B95-8 EBV-infected cells, we detected viral miRNAs as early as day 1 after infection, which reached high levels 5 days post infection (dpi; Fig. 1 E). In RISC-IP, detection of mRNAs was variable among infected B cells of the different donors, a phenomenon that was reported earlier using a related model of established infection and PAR-CLIP experiments (Skalsky et al., 2012; GEO accession no. GSE41437). Therefore, we focused our analyses on candidate mRNAs that were uniformly regulated in all samples (Fig. 1 C), and used RISC-IP results to confirm them (Table S1).

EBV miRNAs inhibit secretion of proinflammatory cytokines and antigen presentation

We confirmed that EBV's miRNAs regulate cytokines central to immune function. Supernatants from B cells infected with the two strains of EBV were assayed for the levels of IL-6, IL-10, TNF, IL12B (IL-12p40), IL-12 (p35/p40), and IL-23 (p19/p40). We added CpG DNA, which stimulates TLR9, for the detection of IL-6 secreted from EBV-infected cells (Iskra et al., 2010). B cells infected with wt/B95-8 EBV secreted less IL-6, TNF, and IL-12p40 than B cells infected with ΔmiR EBV. In contrast, release of the anti-inflamma-

Downloaded from on September 29, 2016

Published September 12, 2016

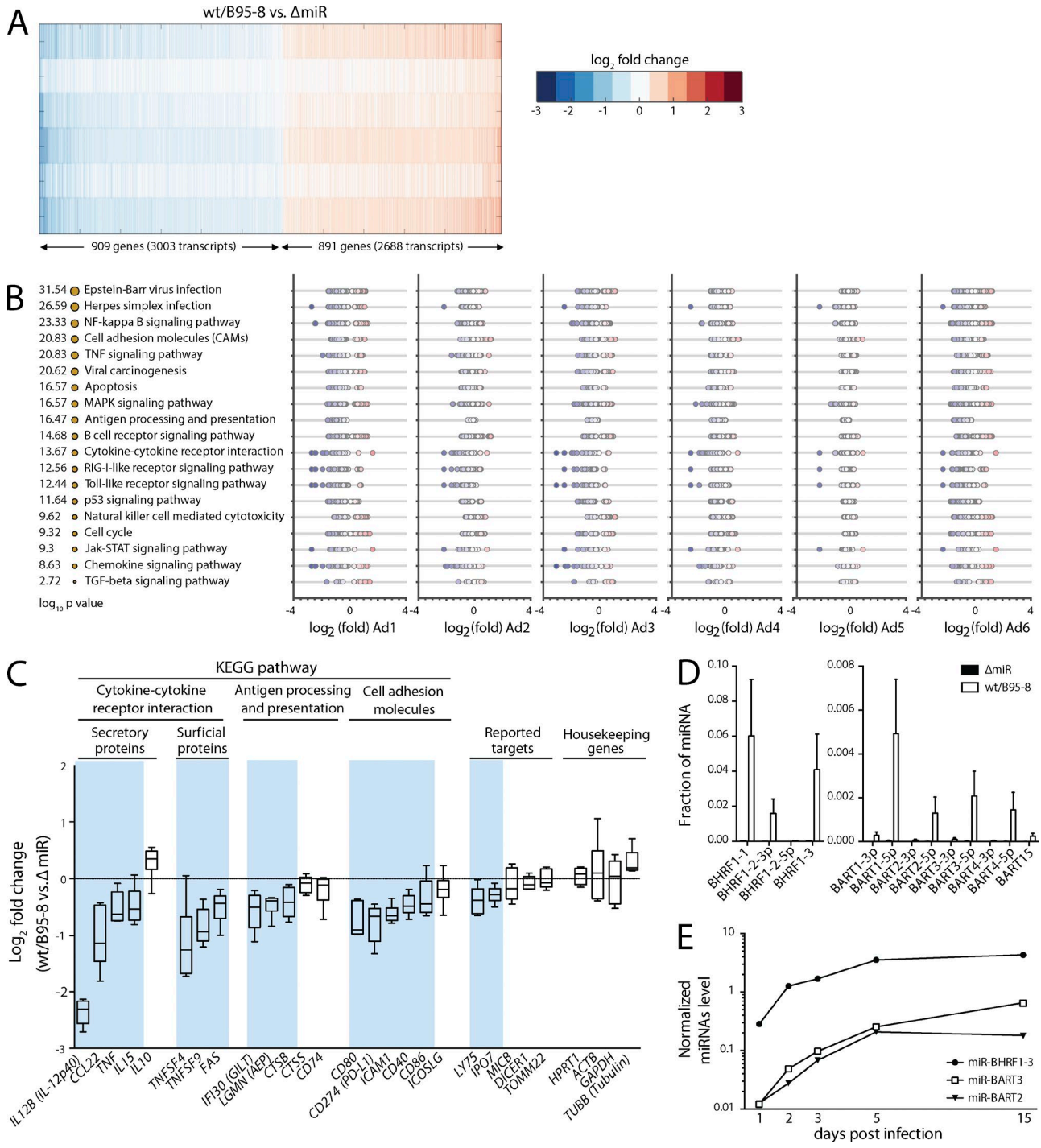

Figure 1. **EBV miRNAs affect major pathways of immunity.** (A) A heat map of the most strongly regulated genes in wt/B95-8 or ΔmiR EBV–infected B cells of six donors (donor Ad1-Ad6) 5 dpi shows differentially expressed gene transcripts with absolute z-scores >1.6. Blue and red indicate down- and up-regulated transcripts, respectively, in wt/B95-8 compared with ΔmiR EBV–infected cells. (B) Shown are gene functions according to KEGG pathway categories with the identified pathways sorted by statistical significance. The sizes of the orange dots indicate $-\log_{10}$ P value scores. For each of the six donors, fold change values of differentially expressed transcripts are plotted. As in A, blue and red indicate down- or up-regulation by EBV miRNAs, respectively. Enrichment of specific pathways was estimated by a hypergeometric distribution test via the KEGG API Web service. (C) Inhibition of selected transcripts associated with adaptive immune responses is shown together with previously reported targets of EBV miRNAs and common housekeeping genes. Blue background shadings indicate genes down-regulated by viral miRNAs (Table S1). (D) Levels of indicated EBV miRNAs in B cells infected with wt/B95-8 or ΔmiR EBV–infected B cells of six donors (donor Ad1-Ad6) 5 dpi were quantified by RISC-IP-seq. Mean ± SD are shown. (E) Three miRNAs, which represent different primary miRNA transcripts in EBV-infected B cells, were quantified with stem-loop qPCR over time. One of two independent experiments is shown.

Downloaded from on September 29, 2016

Published September 12, 2016

tory cytokine IL-10 appeared to be unaffected by viral miRNAs (Fig. 2 A) consistent with our transcriptome analysis (Fig. 1 C). Secretion of IL-12 (p35/p40 or IL-12p70) and IL-23 (p19/p40), both of which contain the IL-12p40 subunit (Szabo et al., 2003), encoded by the *IL12B* gene, was significantly reduced in wt/B95-8 EBV-infected cells compared with ΔmiR EBV-infected cells (Fig. 2 A). Viral miRNAs also inhibited the secretion of IL-12p40 from PBMCs infected with wt/B95-8 EBV (Fig. 2 B). IL-12p40 secretion from PBMCs infected with ΔmiR EBV was reduced when B cells were removed from the PBMCs, indicating that B cells are the main contributors to release of IL-12p40 in PBMCs. Remarkably, our transcriptome analysis revealed the consistent reduction of *IL12B* mRNA with EBV's miRNAs, reducing it by 80% in all six donors' B lymphocytes (Fig. 2 C). Quantitative RT-PCR confirmed this finding (Fig. 2 D).

Multiple EBV miRNAs target *IL12B* and prevent Th1 differentiation of naive CD4$^+$ T cells

We investigated whether *IL12B* was a direct target of EBV miRNAs. EBV's miR-BART1, miR-BART2, and miR-BHRF1-2 repressed the luciferase activity of the *IL12B* reporter (Fig. 3 A). The mutation of predicted binding sites of miR-BART1, miR-BART2, or miR-BHRF1-2 abrogated their ability to inhibit the *IL12B* reporter (Fig. 3 A and Fig. S1), confirming the direct control of *IL12B* by these miRNAs. We similarly analyzed miR-BART10 and miR-BART22, which are present in field strains of EBV but not in wt/B95-8 EBV. For these miRNAs, mutations of their predicted target sites only partially relieved inhibition (Fig. 3 A and Fig. S1), suggesting the presence of additional binding sites in the *IL12B* transcript. In summary, these experiments validated *IL12B* as a direct target of multiple viral miRNAs.

IL-12 is critical for differentiation of Th1 cells (Szabo et al., 2003). Therefore, we co-cultured naive CD4$^+$ T cells with autologous EBV-infected B cells (Fig. 3 B). Relative to ΔmiR EBV, wt/B95-8 EBV-infected B cells repressed Th1 differentiation (Fig. 3, C and D). An antibody that neutralizes the functions of IL12B, but not an isotype control antibody, suppressed Th1 differentiation when T cells were co-cultured with ΔmiR EBV-infected cells (Fig. 3 E), indicating that IL-12, secreted from EBV-infected and activated B cells, was responsible for generation of Th1 cells. Thus, EBV miRNAs suppress the release of IL-12 from infected cells and thereby interfere with formation of Th1 cells, which are important antiviral effectors.

Viral miRNAs directly and indirectly control antigen presentation

Having shown that EBV miRNAs interfere with CD4$^+$ T cell differentiation, we turned our attention to molecules that are involved in recognition of infected cells by specific CD4$^+$ T cells. We quantified levels of surface proteins with a role in HLA class II antigen presentation (Fig. 4). All three subclasses of HLA class II (HLA-DR, HLA-DQ, and HLA-DP) tested were reduced in wt/B95-8 relative to ΔmiR EBV-infected B cells (Fig. 4, A and B), as were many co-stimulatory and adhesion molecules 5 and 15 dpi (Fig. 4 C). MHC class I molecules were also affected, but to a lesser extent.

Among the many co-receptors and adhesion molecules down-regulated in cells infected with wt/B95-8 EBV (Fig. 4 C), we searched for direct targets of EBV miRNAs but found only *CD40* and *FAS* in RISC-IPs (Table S1), which we could not confirm in subsequent luciferase assays using miRNAs encoded by wt/B95-8 EBV. Interestingly, the viral latent membrane protein 1 (LMP1) activates the CD40 pathway, inducing important immune co-receptors (Kieser and Sterz, 2015), but several viral BART miRNAs were reported to control LMP1 expression (Lo et al., 2007; Riley et al., 2012; Verhoeven et al., 2016). We tested these findings in our model of newly infected B cells, and found reduced but highly variable levels of LMP1 transcripts (Fig. 4 D) and protein (Fig. 4 E) in B cells infected with wt/B95-8 EBV compared with ΔmiR EBV 5 dpi. We identified miR-BART3 and miR-BART16 as inhibiting LMP1 in reporter assays (Fig. 4 F). miR-BART3 is encoded in wt/B95-8 EBV, whereas miR-BART16 (Fig. 4 F) is only present in field strains of EBV. We also tested miR-BART1 and miR-BART17, which were reported together with miR-BART16 to target LMP1 3′-UTR (Lo et al., 2007), but failed to confirm that miR-BART1 and miR-BART17 target LMP1 (Fig. 4 F). Collectively, our results showed that viral miRNAs limit LMP1 gene expression and thereby indirectly inhibit surface expression of some immune co-receptors and adhesion molecules.

Viral miRNAs target lysosomal enzymes and inhibit antigen processing

According to our transcriptome analysis, genes encoding lysosomal enzymes actively involved in MHC class II peptide processing (Blum et al., 2013) were inhibited by EBV miRNAs (Fig. 1 C). These included *IFI30* (coding for IFN-γ–regulated thiol reductase GILT), *LGMN* (coding for asparagine endopeptidase AEP alias legumain), and *CTSB* (coding for the peptidase cathepsin B). Expression of all three genes was reduced by EBV miRNAs (Fig. 1 C), which we verified by quantitative RT-PCR (Fig. 5 A). We found that EBV's miR-BART1, miR-BART2, and miR-BHRF1-2 could directly regulate *IFI30*, *LGMN*, and *CTSB* gene expression via their 3′-UTRs in luciferase reporter assays (Fig. 5 B and Fig. S1). Importantly, the knock-down of these three genes (Fig. 5 C) resulted in reduced antigen presentation of exogenously loaded protein (Fig. 5 D). Collectively, our results show that EBV miRNAs interfere with processes involved in MHC class II antigen presentation at multiple levels, including lysosomal protein degradation, HLA class II expression, and co-stimulatory molecule expression.

EBV miRNAs inhibit recognition of infected B cells by EBV-specific CD4$^+$ T cells

Next, we asked whether these multiple levels of regulation ultimately resulted in reduced MHC class II–mediated recognition

Downloaded from on September 29, 2016

Published September 12, 2016

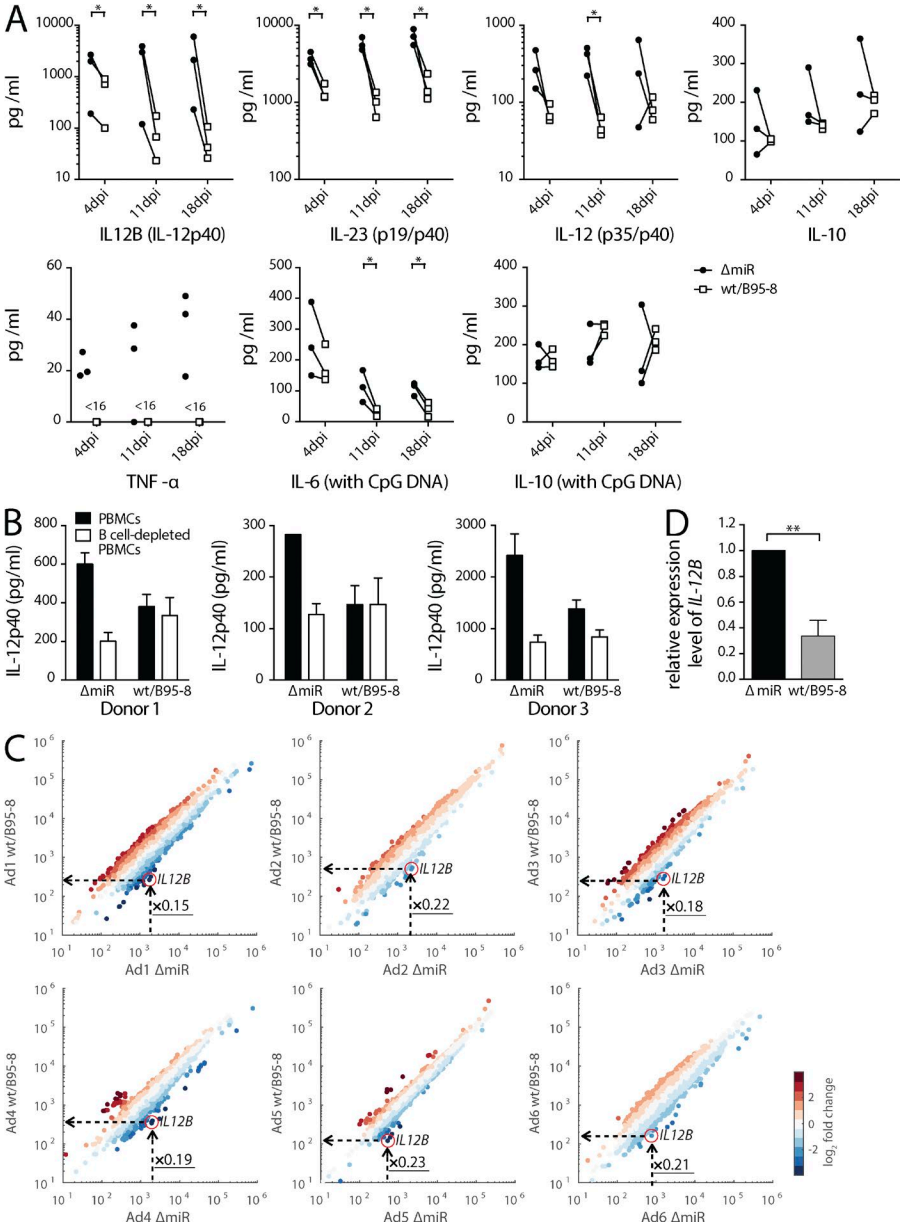

Figure 2. **EBV miRNAs inhibit secretion of proinflammatory cytokines.** (A) B cells infected with wt/B95-8 or ΔmiR EBV for 4, 11, or 18 d were cultivated for an additional 4 d to determine levels of selected cytokines by ELISA (n = 3). CpG DNA was added where indicated. Paired samples from individual donors are connected by solid lines. P values were calculated by a paired two-tailed t test. <16, under the detection limit (16 pg/ml); *, $P < 0.05$. (B) PBMCs or PBMCs depleted of B cells (n = 3) were infected with either wt/B95-8 or ΔmiR EBV, and concentrations of IL-12p40 in the supernatants of the infected B cells after 5 d were determined by ELISA. (C) Shown are scatter plots of transcriptomes of B cells from six donors infected with wt/B95-8 or ΔmiR EBV for 5 d. Fold changes of transcript levels are indicated as blue or red dots, indicating down- and up-regulated transcripts, respectively. The individual *IL12B* transcripts are highlighted by red circles and the calculated fold changes (x-values) are provided. (D) Transcript levels of *IL12B* were measured with quantitative RT-PCR in RNA preparations of B cells infected with wt/B95-8 or ΔmiR EBV for 5 d (n = 4). **, $P < 0.01$.

of EBV-infected cells by antiviral $CD4^+$ T cells. $CD4^+$ T cells from EBV-positive individuals were enriched for EBV-specific T cells by repeated stimulation with irradiated wt/B95-8 EBV-infected autologous LCLs. The EBV-specific $CD4^+$ T cells were then co-cultured with autologous B cells that had been infected with the two EBV strains 5 d earlier (Fig. 6 A, top). Release of IFN-γ by EBV-specific $CD4^+$ T cells was substantial when co-cultured with ΔmiR EBV-infected cells as targets, but was consistently reduced when co-cultured with wt/B95-8 EBV-infected B cells at all cell ratios tested (Fig. 6 B). Activation of EBV-specific $CD4^+$ T cells, measured as IFN-γ release, was observed in autologous and partially matched but not in HLA-mismatched conditions (Fig. 6 C and Table S2), indicating that the activation was HLA class II-restricted.

We also tested an antigen-specific $CD4^+$ T cell clone (Fig. 6, A [bottom] and D) directed against the FGQ peptide, an epitope derived from the viral glycoprotein gp350 (Adhikary et al., 2006). We observed dramatically reduced T cell activities with target B cells infected with wt/B95-8 EBV compared with ΔmiR EBVs 5 dpi (Fig. 6 D). T cell activities were much reduced at 15 dpi, but a difference between wt/B95-8 and ΔmiR EBV-infected target cells remained detectable. Weak recognition on day 15 is in accordance with gp350 protein being delivered as a component of the virion (Adhikary et al., 2006) but not synthesized during prelatency or latency (Kalla et al., 2010). Interestingly, expression of cell surface HLA class II levels peaked between 4 to 10 dpi (Fig. 6 E) suggesting the importance of

Downloaded from on September 29, 2016

Published September 12, 2016

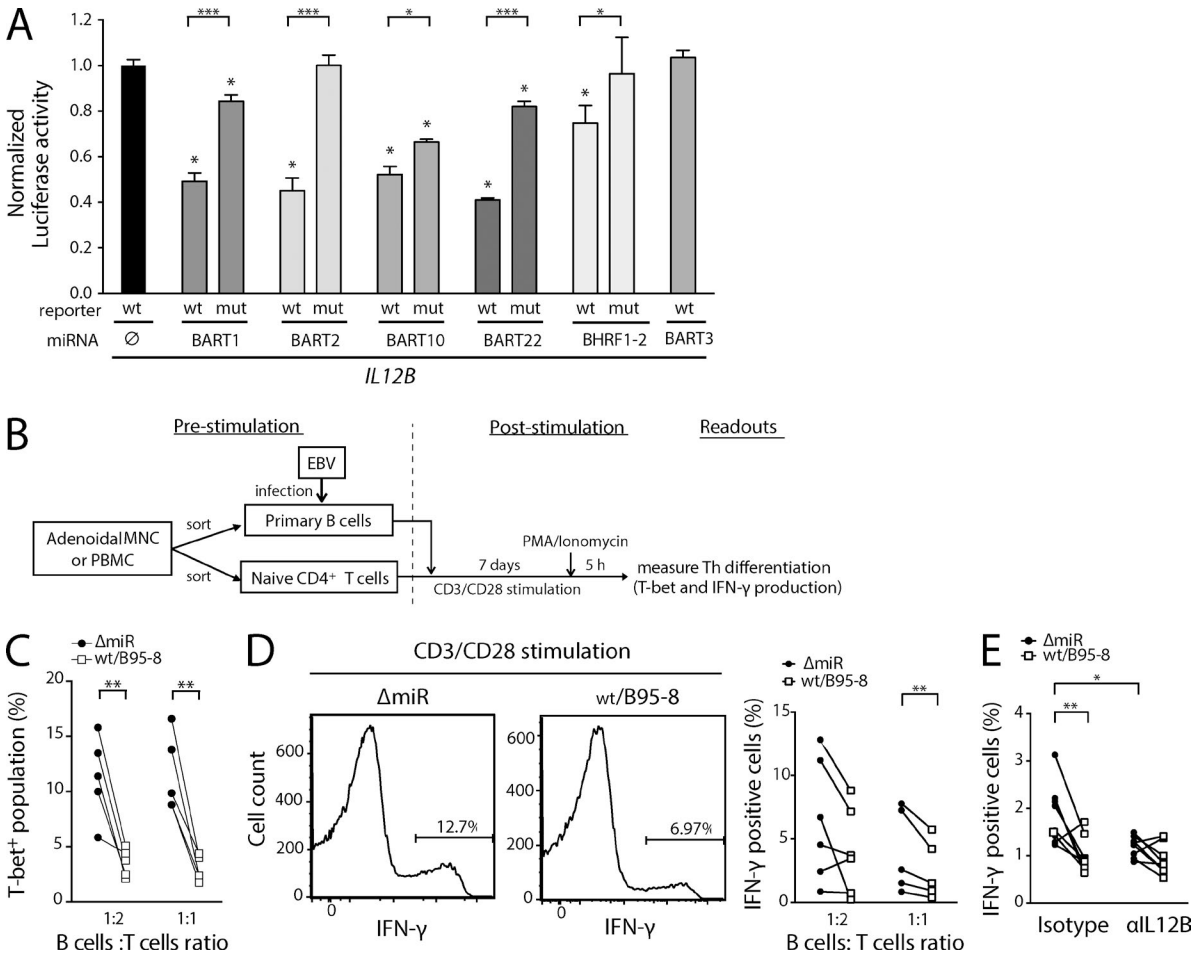

Figure 3. **EBV miRNAs inhibit *IL12B* directly and prevent Th1 differentiation.** (A) HEK293T cells were cotransfected with miRNA expression vectors and luciferase reporter plasmids carrying a wild-type or mutated 3′-UTR (Fig. S2) as indicated ($n = 3$). The luciferase activities were normalized to lysates from cells cotransfected with the wild-type 3′-UTR reporter and an empty plasmid. wt, wild-type 3′-UTR; mut, mutated 3′-UTR; ∅, empty plasmid. P-values were calculated by an unpaired two-tailed Student's *t* test. *, $P < 0.05$; ***, $P < 0.001$, with respect to the luciferase activity of the wild-type reporter cotransfected with empty plasmid. (B) Schematic representation of the steps for experiments shown in C and D. Primary B cells sorted from adenoids or PBMCs were infected with either wt/B95-8 or EBV ΔmiR EBV and co-cultured with autologous naive $CD4^+$ T cells, which were stimulated with αCD3/αCD28 antibody-conjugated beads for 7 d. Th1 differentiation was assessed by intracellular staining of T-bet and IFN-γ after stimulation with PMA/ionomycin for 5 h. (C and D) Naive $CD4^+$ T cells were cultivated for 7 d with autologous, newly infected B cells and αCD3/αCD28 antibody-conjugated beads at indicated ratios ($n = 5$–6). Proliferating PMA- and ionomycin-restimulated Th1 cells were quantified by intracellular T-bet (C) and IFN-γ (D) staining. (D, left) Representative flow cytometry analyses; (right) summary of all experiments. Solid lines indicate paired samples from five to six individual donors. (E) Naive $CD4^+$ T cells were cocultivated with wt/B95-8 or ΔmiR-infected B cells at a B/T cell ratio of 1:1 ($n = 8$) as shown in (B). An anti-IL12B antibody was administered at a concentration of 5 µg/ml, and an irrelevant antibody of the same isotype was used as a control. Solid lines indicate paired samples from individual donors. *, $P < 0.05$; **, $P < 0.01$.

viral miRNAs that counteract $CD4^+$ T cell recognition in the early days of infection.

EBV-specific $CD4^+$ T cells have cytolytic activity (Adhikary et al., 2006). In allogeneic, partially HLA-matched conditions, EBV-specific $CD4^+$ T cells consistently showed stronger cytolysis of target B cells infected with ΔmiR EBV than cells infected wt/B95-8 EBV (Fig. 6 F).

Collectively, we have discovered that EBV miRNAs inhibit the recognition and elimination of infected B cells by HLA class II–restricted $CD4^+$ T cells. Apparently, EBV utilizes multiple miRNAs to interfere with proinflammatory cytokines, antigen processing, and epitope presentation of the infected B lymphocyte to evade EBV-specific and antiviral $CD4^+$ T cells responses early after infection.

DISCUSSION

EBV infects its human hosts for their lifetime, residing in nonproliferating B cells largely invisible to the host's immune response (Thorley-Lawson, 2005). EBV, to be the successful pathogen that it is, however, must both establish a latent in-

Downloaded from on September 29, 2016

Published September 12, 2016

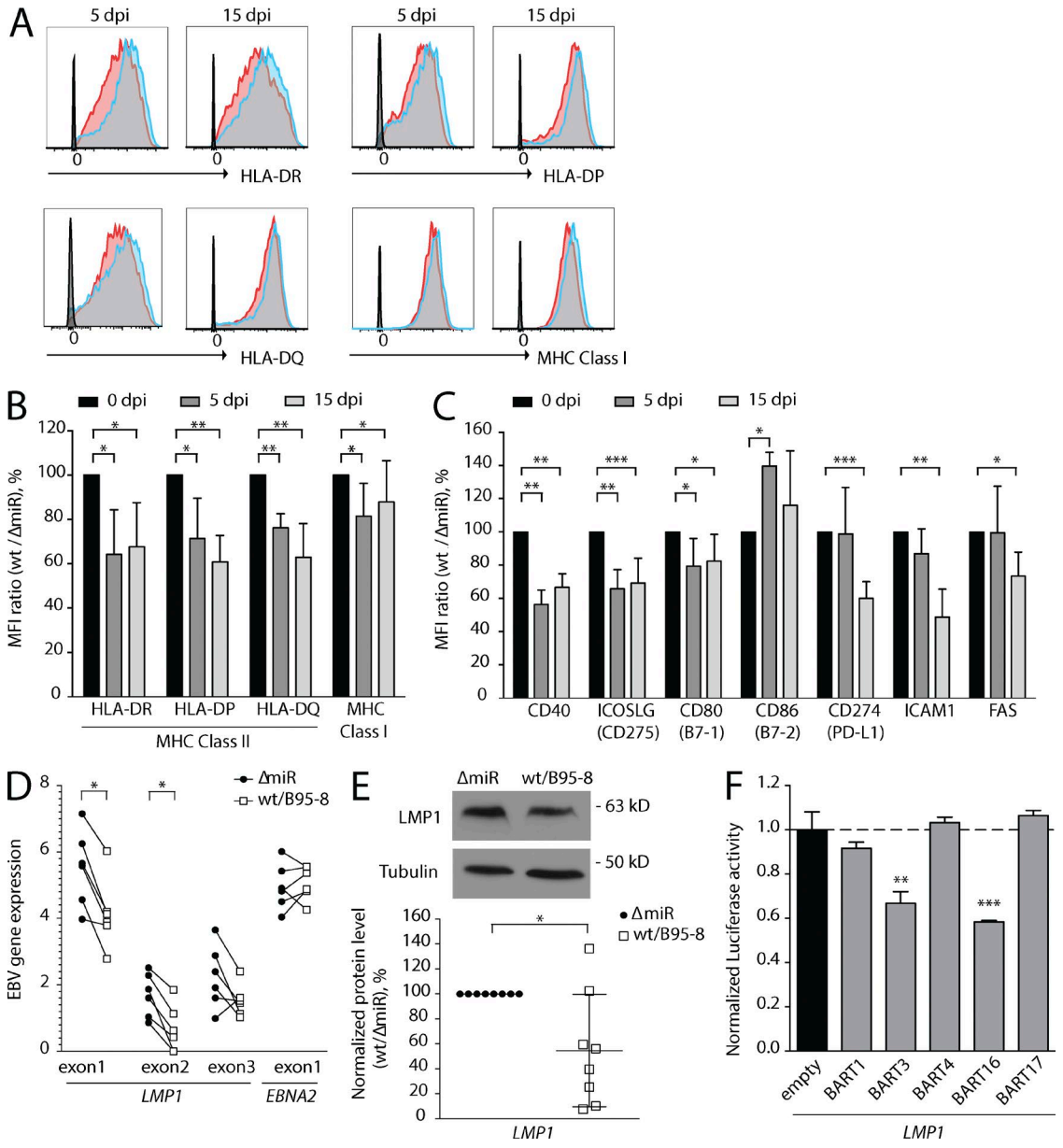

Figure 4. **EBV miRNAs control cell surface levels of HLAs and co-receptors.** (A) FACS panels show the expression profiles of three HLA class II gene families and HLA class I protein on B cells on 5 dpi. One representative example is shown as a histogram for each condition. (B and C) Cell surface expression of HLA molecules (B) and of co-stimulatory and adhesion molecules (C) was measured after immunostaining for proteins inhibited by EBV miRNAs. Ratios (wt/B95-8 divided by ΔmiR EBV–infected B cells) are shown as median fluorescence intensity (MFI). Means ± SD of experiments with infected B cells from 5–10 donors are shown. P-values were calculated by a paired two-tailed Student's *t* test. *, $P < 0.05$; **, $P < 0.01$; ***, $P < 0.001$. (D) Viral gene expression obtained from the transcriptome data shown in Fig. 1 C was quantified for exons to analyze splicing variants precisely. The y-axis shows natural-log values ($n = 6$) with paired samples from individual donors connected by solid lines. Statistical significance was assessed with the repeated-measurements ANOVA. *, adjusted $P < 0.01$. (E) Cell lysates were prepared from B cells infected with wt/B95-8 or ΔmiR EBV for 5 d and analyzed by Western blotting for expression of LMP1 and tubulin. An example (top) and the quantification of all results (bottom) are shown. Protein levels were measured relative to tubulin and LMP1 levels in ΔmiR EBV-infected cells were set to 100%. Mean ± SD are shown ($n = 8$). (F) Dual luciferase reporter assays with LMP1 3′-UTR are shown ($n = 3$). P-values were calculated by an unpaired two-tailed Student's *t* test. *, $P < 0.05$; **, $P < 0.01$; ***, $P < 0.001$.

fection and produce and disseminate progeny virus, all in the face of robust innate and adaptive immune responses.

Such responses include EBV-specific $CD4^+$ T cells, which have an important role in controlling EBV infection and disease. For example, patients with EBV-associated tumors treated with virus-specific T cell preparations showed better clinical responses if the preparations contained larger fractions of $CD4^+$ T cells (Haque et al., 2007; Icheva et al.,

Downloaded from on September 29, 2016

Published September 12, 2016

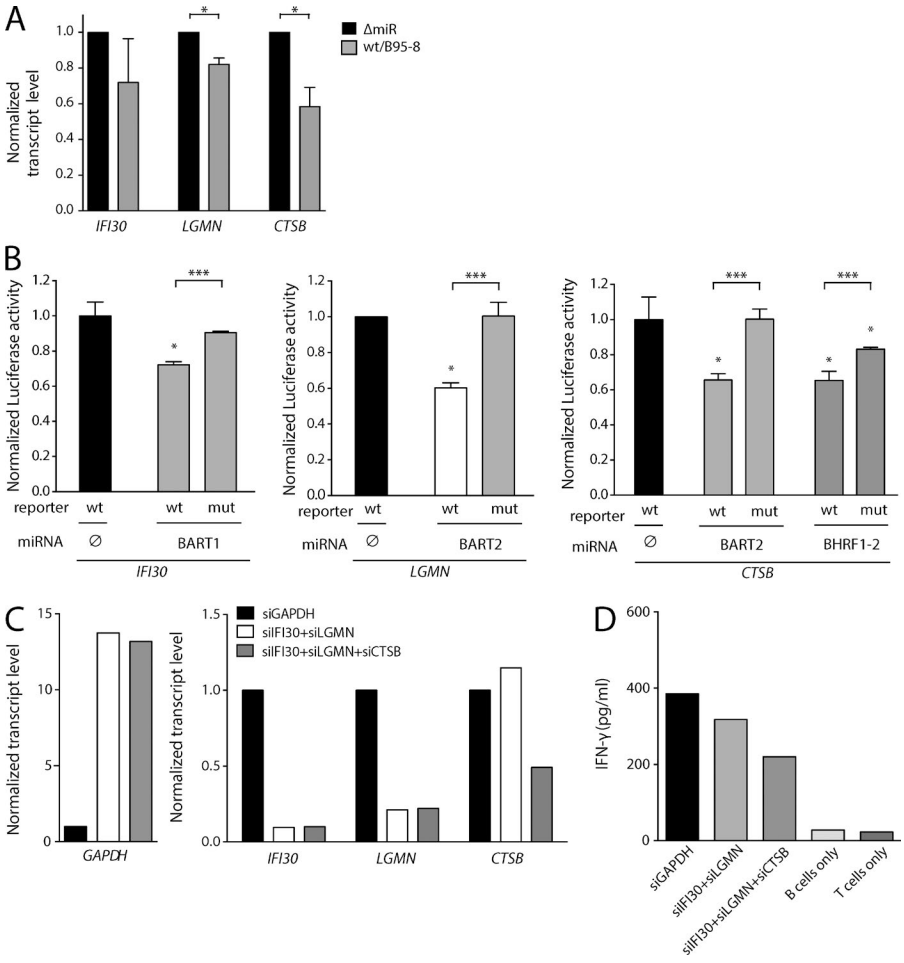

Figure 5. **Viral miRNAs inhibit two lysosomal endopeptidases and a thiol reductase needed for antigen presentation.** (A) Transcript levels of *IFI30*, *LGMN*, and *CTSB* encoding GILT, AEP, and CTSB, respectively, were measured with quantitative RT-PCR (n = 3). P-values were calculated by a paired two-tailed Student's t test. *, $P < 0.05$. (B) HEK293T cells were cotransfected with different miRNA expression vectors and luciferase reporter plasmids carrying 3′-UTRs as indicated (n = 3). The luciferase activities were normalized to lysates from cells cotransfected with the wild-type 3′-UTR reporter and an empty plasmid. wt, wild-type 3′-UTR; mut, mutated 3′-UTR; ∅, empty plasmid. P-values were calculated by an unpaired two-tailed Student's t test. *, $P < 0.05$; ***, $P < 0.001$, with respect to the luciferase activity of the wild-type reporter cotransfected with an empty expression plasmid. (C) Transcript levels after RNAi knock-down of lysosomal enzyme-encoding genes were investigated. DG-75 cells were transduced with commercial siRNAs directed against *GAPDH*, *IFI30*, *LGMN*, or *CTSB* as indicated and transcript levels were quantified with RT-PCR. Means of three technical replicates are shown. (D) DG-75 cell transduced with siRNAs directed against three lysosomal enzymes as in (C) were loaded with purified influenza M1 protein and co-cultured with M1-specific $CD4^+$ T cells (epitope LENL; HLA-DRB1*1301-restricted) for 1 d. After another 16 h, IFN-γ secretion was assessed by ELISA. One of two independent experiments is shown as means of three technical replicates.

2013). $CD4^+$ T cells target a wide repertoire of EBV antigens from all phases of latent and lytic infection (Adhikary et al., 2007; Long et al., 2011). $CD4^+$ T cells with specificity for structural EBV proteins play a prominent role: they are a universal component of the T cell repertoire, rapidly detecting EBV-infected B cells and killing them directly (Adhikary et al., 2006, 2007). Several EBV proteins expressed during its lytic phase can inhibit recognition of EBV-infected cells by $CD4^+$ T cells (Ressing et al., 2015). The broad-ranging functions of the host shut-off gene product BGLF5 include reduction of HLA class II molecules on the cell surface during EBV's lytic, productive phase (Rowe et al., 2007). The late glycoprotein gp42, encoded by BZLF2, was shown to associate with HLA class II and to hinder recognition by $CD4^+$ T cells sterically (Ressing et al., 2003). Both mechanisms are unlikely to be operational in newly infected B lymphocytes, because the two viral proteins appear not to be expressed in the prelatent phase (Kalla et al., 2010). Viral IL-10, encoded by BCLF1, is an immunomodulatory protein expressed early in infection, but its effects on B cell elimination by $CD4^+$ T cells were limited (Jochum et al., 2012). Two additional viral gene products reported to affect $CD4^+$ T cell recognition, BDLF3 (Quinn et al., 2015) and BZLF1 (Zuo et al., 2011), may act during EBV primary infection, because BDLF3 is in the virus particle (Johannsen et al., 2004) and BZLF1 has been found to be expressed early during infection (Wen et al., 2007; Kalla et al., 2010). BDLF3 transcripts were present at very low levels, only, whereas BZLF1 transcripts were not mapped in our RNA-Seq analysis. Thus, how EBV infection escapes detection and elimination by EBV-specific T cells during the early phase of infection has remained uncertain.

Here, we present an answer to this question and show that EBV uses its large repertoire of miRNAs to target $CD4^+$ T cell differentiation and recognition of infected cells. It appears that EBV's immunoevasive strategy uses miRNAs, which are themselves nonimmunogenic (Boss and Renne, 2011), rather than viral proteins which themselves would be antigenic. EBV induces a state of reduced immunogenicity in infected and recently activated B cells with viral miRNAs, which allows the virus to express its latency-associated antigens avoiding the recognition and elimination by $CD4^+$ T cells. Because activated B cells are professional antigen-pre-

Downloaded from on September 29, 2016

Published September 12, 2016

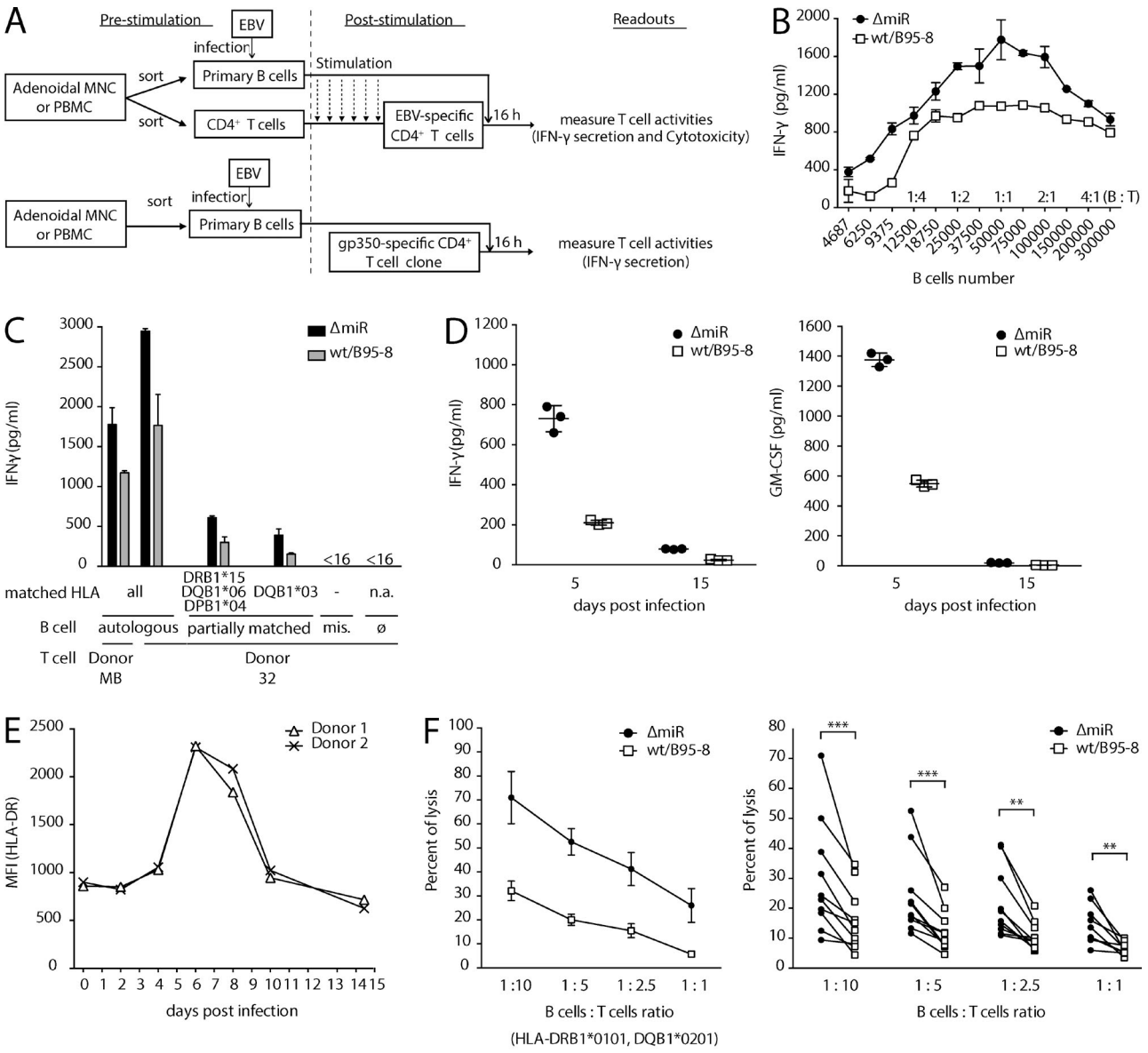

Figure 6. **EBV miRNAs inhibit recognition and killing of infected B cells by EBV-specific CD4⁺ T cells.** (A) Overview of the co-culture experiments used in B–F. Primary B cells sorted from adenoids or PBMCs were infected with either wt/B95-8 or ΔmiR EBV and co-cultured with polyclonal (top) or monoclonal (bottom) EBV-specific CD4⁺ T cells. Polyclonal antiviral CD4⁺ T cells were selected through stimulation (once in every two weeks) with irradiated LCLs infected with wt/B95-8 EBV. (B) Polyclonal EBV-specific CD4⁺ T cells were co-cultured for 16 h with autologous B cells that had been infected 5 d earlier. Levels of secreted IFN-γ were quantified by ELISA ($n = 3$). Several B/T cell ratios were used as indicated. Means ± SD are shown. (C) Autologous, partially HLA-matched, or mismatched (mis.) B cells infected with wt/B95-8 or ΔmiR EBV ($n = 3$; Table S2) were cocultivated with polyclonal EBV-specific CD4⁺ T cells and secreted IFN-γ was quantified by ELISA after 16 h. The B/T cell ratio was 1:1. Matched HLA class II alleles are indicated. Means ± SD are shown. <16 is under the detection limit (16 pg/ml); ∅, only T cells; n.a., not applicable. (D) The gp350-specific CD4⁺ T cell clone, epitope FGQ (HLA-DRB1*1301), was used as effector cells together with autologous B cells from donor JM (Table S2) as targets. B cells had been infected for 15 d with the two EBV strains as indicated and were used at an B/T cell ratio of 1:1. After 16 h of co-culture, levels of secreted IFN-γ and GM-CSF were quantified by ELISA. Means ± SD are shown. (E) MFIs measured in flow cytometry analysis of cell surface HLA-DR in primary B cells infected with wt/B95-8 EBV from two different donors were calculated. (F) Killing of EBV-infected B cells by EBV-specific CD4⁺ T cells was analyzed at various B/T cell ratios by Calcein release assays. A representative experiment with partially matched EBV-infected target B cells (left; $n = 3$) and a summary of all independent experiments with partially matched B cells (right) are shown. Paired samples from individual donors are connected by solid lines. Means ± SD are shown. P-values were calculated by a paired two-tailed Student's t test. **, $P < 0.01$; ***, $P < 0.001$.

Downloaded from on September 29, 2016

Published September 12, 2016

senting cells and express multiple immune-activating molecules (Wiesner et al., 2008), the need for EBV to control its host cell is more urgent than for other complex viruses that do not rely on professional antigen-presenting immune cells for their life-cycle.

In our experiments, recognition of early-stage infected B cells by $CD4^+$ T cells was strongly inhibited by multiple mechanisms, pointing to the biological importance of the immunoevasive functions of viral miRNAs. First, *IL12B* is dramatically repressed in wt/B95-8 EBV-infected B cells compared with ΔmiR EBV-infected B cells, leading to the down-regulation of three IL-12 family cytokines, IL-12B (IL-12p40), IL-12 (p35/p40), and IL-23 (p19/p40). At least five different viral miRNAs control the fate of the *IL12B* transcript, targeting multiple sites within its 3′-UTR, indicating its critical role in immune regulation by EBV-infected B cells and a redundancy or even cooperativity of viral miRNAs. Interestingly, the miRNAs controlling *IL12B* originate from different viral transcripts (Barth et al., 2011), suggesting a robust control of *IL12B* in all phases of EBV's life cycle and in the many cell types EBV infects, which show different patterns of miRNA expression (Cai et al., 2006; Qiu et al., 2011). Repression of *IL12B* may not only reduce $CD4^+$ T cell differentiation, as shown here, but also regulate T cell effector functions (Curtsinger and Mescher, 2010).

Second, lysosomal proteolysis is regulated. Transcripts of lysosomal endopeptidases, AEP and CTSB, and a thiol reductase, GILT, which are involved in proteolytic degradation and HLA class II epitope generation (Blum et al., 2013), are direct targets of the miRNAs miR-BART1, miR-BART2, and miR-BHRF1-2. An siRNA-mediated knock-down of these three genes in human B cells reduced their recognition by clonal epitope-specific $CD4^+$ T cells (Fig. 5, C and D; Milosevic et al., 2005) suggesting an important role of the three lysosomal enzymes in antigen processing and presentation via MHC class II molecules in human B cells.

Third, HLA class II surface levels are down-regulated in B cells infected with wt/B95-8 EBV (Fig. 4 B). We also tested if EBV miRNA targeted MHC class II molecules directly. miRNAs encoded in wt/B95-8 EBV failed to inhibit consistently four HLA-DRB1 alleles tested in dual luciferase reporter assays and also lacked functional miRNA-binding sites. Thus, the reduction of HLA class II molecules is likely indirect and may be a consequence of altered lysosomal processing of epitopes. Such phenomena might be particularly important early during infection when the EBV-activated B cells present antigenic peptides of virion components (Fig. 6 D) and the expression of HLA class II molecules peaks at the cell surface (Fig. 6 E). Together, these findings demonstrate that EBV miRNAs redundantly and robustly inhibit specific immune functions in newly infected B cells that may otherwise metabolize viral proteins into HLA class II-presented peptides for recognition by antiviral $CD4^+$ T cells.

A limited number of observations have been made before on immunomodulatory functions of EBV miRNAs. The RNAs encoding the innate immune effector molecules *MICB* (Nachmani et al., 2009) and *NLRP3* (Haneklaus et al., 2012) have been found in cell lines to be inhibited by EBV's miRNAs. They were not down-regulated in our experiments (Fig. 1 C, Table S1, and GSE75776), which examined their levels during early infection of primary B cells. Our studies with primary B cells likely avoided the adaptive changes that arise during long-term culturing in vitro.

It is not immediately apparent why B lymphocytes release proinflammatory cytokines upon infection with EBV. One explanation is based on two viral, noncoding RNAs, termed EBERs, which are contained in virions and are transcribed in all EBV-infected cells. EBERs are known to trigger the endosomal TLR3 receptor or the cytosolic RIG-I sensor signaling pathway and induce type I interferon and IL-6 synthesis in infected B cells (Samanta et al., 2006; Wu et al., 2007; Iwakiri et al., 2009), which might lead to the expression of proinflammatory cytokines found in higher concentrations in the supernatants of B cells infected with ΔmiR than with wt/B95-8 EBV.

Interestingly, LMP1, a viral membrane protein that is predominantly expressed in the latent phase but also early upon B cell infection, activates the CD40 pathway, and induces IL-6, adhesion molecules, and important immune co-receptors (Kieser and Sterz, 2015). Several viral BART miRNAs have been reported to control LMP1 expression (Lo et al., 2007; Verhoeven et al., 2016). We confirmed that miR-BART16, which is not in the wt/B95-8 EBV strain, and miR-BART3, which was not previously known to target LMP1 directly, do target it (Fig. 4 F). In addition, miR-BART3 was recently reported to reduce LMP1 protein levels in HEK 293T cells (Verhoeven et al., 2016). We failed to identify direct targets among the many co-receptors and adhesion molecules down-regulated in cells infected with wt/B95-8 EBV (Fig. 4 C). It is possible that, on average, BART miRNAs repress LMP1 levels in cells infected with wt/B95-8 EBV, and thereby indirectly inhibit surface expression of some immune co-receptors and adhesion molecules, further reducing immune recognition of EBV-infected B lymphocytes.

EBV induces proliferation of the B cells it initially infects, and fosters their survival. We have found that EBV encodes miRNAs that regulate multiple facets of a host's adaptive immune response in newly infected B cells. EBV-infected B cells lacking viral miRNAs are deficient both in regulating these responses and in other miRNA-dependent functions, including an inhibition of apoptosis (Seto et al., 2010). These latter defects have precluded comparisons of B cells newly infected with wt/B95-8 or ΔmiR in humanized mouse models. In infection experiments with these mice, we observed defects in persistence after infection with ΔmiR EBV compared with wt/B95-8 EBV, possibly resulting from a combination of decreased survival and enhanced immune control (unpublished data; C. Münz, personal communication).

Collectively, our studies of a model that closely mimics physiological infection in the early phase show that EBV's miRNAs interfere with $CD4^+$ T cell control through multiple mechanisms. They inhibit the secretion of cytokines,

Downloaded from on September 29, 2016

Published September 12, 2016

inhibit antigen processing and presentation, inhibit the differentiation of $CD4^+$ T cells, and counteract recognition and elimination of infected B cells by EBV-specific $CD4^+$ effector T cells. The breadth of EBV's use of its miRNAs to inhibit adaptive immune responses is unprecedented and contributes to its efficient establishment of a lifelong infection.

MATERIALS AND METHODS

Patient samples

Surgically removed adenoids and PBMCs were obtained from anonymous patients and anonymous volunteer blood donors, respectively, from Munich, Germany. The use of this human material was approved by the local ethics committee (Ethikkommission bei der LMU München) in writing.

Separation of human primary cells

Human primary B and T cells were prepared from adenoidal mononuclear cells (MNCs) or PBMCs by Ficoll-Hypaque gradient centrifugation with Pancoll (PAN-Biotech). B cells, $CD4^+$ T cells, $CD8^+$ T cells, and naive $CD4^+$ T cells were separated from adenoidal MNCs or PBMCs using MACS separator (Miltenyi Biotec) with CD19 MicroBeads, CD4 MicroBeads, CD8 MicroBeads, and Naive $CD4^+$ T cell Isolation kit II, respectively.

Cell lines and cell culture

Burkitt's lymphoma cell lines Raji (EBV-positive), DG-75 (EBV-negative), HEK293-based EBV producer cell lines (Seto et al., 2010), infected human primary B cells, and T cells were maintained in RPMI-1640 medium (Thermo Fischer Scientific). HEK293T cells were maintained in DMEM medium. All media were supplemented with 10% FBS (Thermo Fischer Scientific), penicillin (100 U/ml; Thermo Fischer Scientific), and streptomycin (100 mg/ml; Thermo Fischer Scientific). Cells were cultivated at 37°C in a 5% CO_2 incubator.

Preparation of infectious EBV stocks and infection of human primary B cells

Infectious EBV stocks were prepared as previously described (Seto et al., 2010). In brief, EBV producer cell lines for ΔmiR (p4027) and wt/B95-8 (p2089) EBV strains were transiently transfected with expression plasmids encoding BZLF1 and BALF4 to induce EBV's lytic cycle. We collected supernatants 3 d after transfection, and debris was cleared by centrifugation at 3,000 rpm for 15 min. Virus stocks were titrated on Raji cells as previously reported and used at a multiplicity of infection (MOI) of 0.1 Green Raji units (Seto et al., 2010) for infecting primary B lymphocytes with an optimal virus dose (Steinbrück et al., 2015). For virus infection, primary B cells were cultivated with each virus stock for 18 h. After replacement with fresh medium, the infected cells were seeded at an initial density of 5×10^5 cells per ml.

RNA-Seq and RISC-IP

At 5 dpi of human primary B cells, we extracted total RNAs with TRIzol (Thermo Fischer Scientific) and Direct-Zol RNA MiniPrep kit (Zymo Research) from six different donors (Ad1–Ad6; Fig. 1) for RNA-Seq, according to the manufacturers' protocols. In parallel, we performed RISC immunoprecipitation (RISC-IP) as described previously (Kuzembayeva et al., 2012). In brief, lysed cells were incubated with anti-Ago2 antibody (11A9)-conjugated Dynabeads (Thermo Fischer Scientific), washed, and coprecipitated RNA was extracted. The cDNA libraries were prepared (Vertis Biotechnologie AG). For RNA-Seq, total RNAs were depleted of rRNAs by Ribo-Zero rRNA Removal kit (Illumina), fragmented by ultrasonication, and subjected to first strand synthesis with a randomized primer. For RISC-IP, RNAs were poly (A)-tailed, ligated with an RNA adapter at 5′-phosphates to facilitate Illumina TruSeq sequencing, and subjected to first strand synthesis with an oligo-(dT) primer. The cDNAs were PCR-amplified and sequenced with an Illumina HiSeq2000 instrument at the University of Wisconsin Biotechnology Center DNA Sequencing Facility.

Analysis of deep sequencing

For RNA-Seq, processing of paired-end reads (poly-A tail filtering, N-filtering, and adapter removal) was done using FastQC and R2M (RawReadManipulator). Reads were mapped to the human genome (hg19 'core' chromosome-set) by STAR (Dobin et al., 2013) and feature counts per transcript were determined using featureCounts and GENCODE version 19 annotations, together with EBV's annotation (available from GenBank under accession no. AJ507799). To screen differentially regulated genes by viral miRNAs, we used a simple but efficient scoring algorithm based on donor/replicate-wise fold changes ranks. For each gene g and replicate k, we calculate the gene-specific rank score as

$$r_g = \frac{1}{m}\sum_{k=1}^{n} r_{gk},$$

where n is the number of all replicates, m the number of all genes/transcripts, and r_{gk} is the rank of gene g in sample k. To select highly differentially expressed genes, we transformed the rank score into a z-score and selected all transcripts with an absolute z-score >1.6.

For RISC-IP the mapped reads were normalized using size factors estimated with the R package DEseq2 and filtered for reads mapped to annotated 3′-UTR regions using GENCODE version19. To identify local quantitative differences in the read enrichments on 3′-UTRs between wt EBV compared with ΔmiR EBV-infected B cells, we calculated a donor-wise relative enrichment score. For each genomic position p, the relative expression es_p was calculated as

$$es_p = \frac{e_{tp}}{e_{tp} + e_{cp}} \times n_{pu},$$

where e_{tp} is the enrichment value of sequenced reads at position p in wt/B95-8 EBV-infected cells and e_{cp} the local enrichment value in ΔmiR EBV-infected B cells, respectively.

Downloaded from on September 29, 2016

Published September 12, 2016

The normalization factor $n_{pu} = e_{tp}/max(e_u)$ was introduced to correct for local maxima in the UTR sequence of interest, where $max(e_u)$ is the maximum enrichment value in the UTR sequence u. Finally, we used a Gaussian filter to minimize local noise. To select 3′-UTRs bound by viral miRNAs, we set the threshold as follows: enrichment score >0.6 for a stretch of >20 nt in the 3′-UTRs in two or more donors. To quantify viral miRNAs incorporated into the RISC in infected cells, we mapped reads from the RISC-IP Seq to miRNA entries registered in miRBase 21 and calculated fractions of each viral miRNAs out of total miRNA read counts.

KEGG enrichment pathway

Enrichment of specific pathways was estimated by performing a hypergeometric distribution test via the KEGG API Web Service. All calculations were done using Matlab (Mathworks).

ELISA

To detect cytokine secretion from infected B cells, 10^6 cells were seeded in 6-well plates at 4 or 11 dpi, cultivated for 4 d with cyclosporine (1 µg/ml; Novartis). Supernatants were harvested and stored at −20°C. ELISAs for IL-6, IL-10, IL12B (IL-12p40), IL-12, IL-23, and TNF were performed following the manufacturer's protocols (Mabtech). For IL-6 and IL-10, CpG DNA were added as previously described (Iskra et al., 2010) to stimulate infected B cells. ELISA for IFN-γ levels was performed following the manufacturer's protocol (Mabtech).

To detect IL-12p40 secretion from PBMCs or PBMCs depleted of B cells using the MACS separator and CD19 MicroBeads (Miltenyi Biotec), the cells were infected with either wt/B95-8 or ΔmiR EBV at MOIs of 0.1 Green Raji units (Steinbrück et al., 2015). After 5 d of incubation, supernatants were collected and ELISA for IL-12p40 levels was assessed following the manufacturer's protocol (Mabtech).

Luciferase reporter assays

The 3′-UTRs of *IL12B* (Ensembl ENST00000231228), *IFI30* (Ensembl ENST00000407280), *LGMN* (Ensembl ENST00000334869), *CTSB* (Ensembl ENST00000353047), and LMP1 (available from GenBank under accession no. AJ507799) were cloned downstream of Renilla luciferase (*Rluc*) in the expression plasmid psiCHECK-2 (Promega). To construct the viral miRNA expression vectors, we cloned TagBFP (Evrogen) under the control of the EF1α promoter into pCDH-EF1-MCS (System Biosciences). Single miRNAs of interest were cloned downstream of the TagBFP-encoding gene. Viral miRNAs were obtained by PCR from the p4080 plasmid (Seto et al., 2010). 50 ng of the psiCHECK-2 reporter and 150 ng of the pCDH-EF1 miRNA expressor plasmid DNAs were cotransfected into 1×10^5 HEK293T cells by Metafectene Pro (Biontex). After 24 h of transfection, we measured luciferase activities with the Dual-Luciferase Assay kit (Promega) and the Orion II Microplate Luminometer (Titertek-Berthold). The activity of Rluc was normalized to the activity of Fluc (Firefly luciferase) encoded in the psiCHECK-2 reporter plasmid. We performed in silico prediction of EBV miRNA-binding sites on 3′-UTRs primarily with TargetScan (Garcia et al., 2011) and used RNAhybrid (Rehmsmeier et al., 2004) to screen for 6mer binding sites (Bartel, 2009). We performed site-directed mutagenesis with overlapping oligo DNAs and Phusion polymerase (NEB).

Quantitative RT-PCR

To quantify mRNA levels RNAs were reverse-transcribed with SuperScript III Reverse transcription (Thermo Fischer Scientific) and quantitative PCR was performed with LightCycler 480 SYBR Green I Mix (Roche) and LightCycler 480 Instrument II (Roche) according to the manufacturers' instructions. The following primers were used for the detection: *HPRT1* 5′-TGACCTTGATTTATTTTGCATACC-3′ and 5′-CGAGCAAGACGTTCAGTCCT-3′; *HMBS* 5′-CTGAAAGGGCCTTCCTGAG-3′ and 5′-CAGACTCCTCCAGTCAGGTACA-3′; *IL12B* 5′-CCCTGACATTCTGCGTTCA-3′ and 5′-AGGTCTTGTCCGTGAAGACTCTA-3′; *IFI30* 5′-CTGGGTCACCGTCAATGG-3′ and 5′-GCTTCTTGCCCTGGTACAAC-3′; *LGMN* 5′-GGAAACTGATGAACACCAATGA-3′ and 5′-GGAGACGATCTTACGCACTGA-3′; *CTSB* 5′-CTGTGGCAGCATGTGTGG-3′ and 5′-TCTTGTCCAGAAGTTCCAAGC-3′.

To quantify miRNA levels, stem-loop qPCRs were performed with TaqMan MicroRNA Reverse Transcription kit (Thermo Fischer Scientific) and TaqMan Universal Master Mix II (Thermo Fischer Scientific) according to the manufacturer's protocols. *RNU6B* was used for normalization. Following TaqMan MicroRNA assays, specific primers (Thermo Fischer Scientific) were used for detection: ebv-miR-BART2: 197238_mat; ebv-miR-BART3: 004578_mat; ebv-miR-BHRF1-3 197221_mat; *RNU6B*: 197238_mat.

Establishment of EBV-specific effector T cells and T cell clones

EBV-specific $CD4^+$ T cell clones were established from polyclonal T cell lines that were generated by LCLs or mini-LCL stimulation of PBMCs, as previously described (Adhikary et al., 2007).

Flow cytometry and antibodies

After immunostainings with fluorophore-conjugated antibodies, single-cell suspensions were measured with LSRFortessa or FACSCanto (BD) flow cytometers and the FACSDiva software (BD). Acquired data were analyzed with FlowJo software Ver. 9.8 (FlowJo). The following fluorophore-conjugated antibodies reactive to human antigens were used: anti–human IFN-γ APC (4S.B3, IgG1; BioLegend), anti-CD40 PE (5c3, IgG2b; BioLegend), anti–ICOS-L (B7-H2) PE (2D3, IgG2b; BioLegend), anti–PD-L1 (B7-H1) APC (29E.2A3, IgG2b; BioLegend), anti-CD86 (B7-2) PE (37301, IgG1; R&D Systems), anti-CD54 (ICAM-1) APC (HCD54, IgG1; BioLegend), anti–HLA-ABC APC (W6/32, IgG2a;

Downloaded from on September 29, 2016

Published September 12, 2016

BioLegend), anti-CD80 PE-Cy5 (L307.4; BD), anti-FAS (CD45) PE (Dx2, IgG1; BioLegend), anti–HLA-DR unlabeled (L234, IgG2a; BioLegend), anti–HLA-DQ unlabeled (SPV-L3, IgG2a ; AbD Serotec), anti–HLA-DP unlabeled (B7/21, IgG3; Abcam), anti–mouse F(ab')2 APC (polyclonal, IgG; eBioscience), isotype IgG1 PE (MOPC-21; BioLegend), isotype IgG2b PE (MPC-11; BioLegend), isotype IgG1 APC (MOPC-21; BD), isotype IgG2a APC (MOPC-173; BioLegend), and isotype IgG2b APC (MG2b-57; BioLegend).

Western blotting

We lysed cells with RIPA buffer (50 mM Tris-HCl, pH 8.0, 150 mM NaCl, 0.1% SDS, 1% NP-40, and 0.5% DOC) and boiled the extracts with Laemmli buffer. Proteins were separated on SDS-PAGE gels (Carl Roth) and transferred to nitrocellulose membranes (GE Healthcare) using Mini-PROTEAN Tetra Cell (Bio-Rad Laboratories). Membranes were blocked for 30 min with Roti-Block (Carl Roth), followed by antibody incubation. Secondary antibodies conjugated with horseradish peroxidase were used (Cell Signaling Technology) and exposed to CEA films (Agfa HealthCare). Protein levels were quantified with the software ImageJ. The following primary antibodies reactive to human proteins were used: anti–human Tubulin (B-5-1-2; Santa Cruz Biotechnology, Inc.). The monoclonal antibody (1G6-3) reactive to the EBV protein LMP1 was provided by E. Kremmer (Institute of Molecular Immunology, Helmholtz Zentrum München, München, Germany).

RNAi knock-down and recognition by M1-specific CD4$^+$ T cells

4×10^5 DG-75 cells were incubated in 1 ml Accell Delivery Media (GE Healthcare) and 1 nmol siRNAs directed against *GAPDH*, *IFI30*, *LGMN*, *CTSB,* or combinations thereof for 48 h. Influenza M1 protein purified as previously described (Nimmerjahn et al., 2003) was added to the medium, and the cells were further incubated for 24 h and co-cultured with M1-specific CD4$^+$ T cell clone E5 for 16 h (Milosevic et al., 2005). IFN-γ levels were detected with ELISA.

T cell differentiation and recognition

Th1 differentiation was assessed by co-culture of sorted naive CD4$^+$ T cells and infected B cells 5 dpi. 1×10^5 naive CD4$^+$ T cells stained with CellTrace Violet (Thermo Fischer Scientific) and 0.5 or 1×10^5 infected B cells were cultured in 96-well plates with Dynabeads Human T-Activator CD3/CD28 (Thermo Fischer Scientific) and cultivated for 7 d. The neutralizing antibody against IL12B (C8.6; BioLegend) or the corresponding isotype control antibody (MOPC-21; BioLegend) were added for certain experiments at 5 µg/ml. Cells were restimulated with PMA and ionomycin (Cell Stimulation Cocktail; eBioscience) for 5 h and treated with Brefeldin A and Monensin (BioLegend) for 2.5 h before fixation. Th1 population was measured by intracellular IFN-γ staining with FIX and PERM Cell Fixation and Cell Permeabilization kit (Thermo Fischer Scientific) and subsequent flow cytometry analysis. The Th1 population was defined as IFN-γ$^+$ T cells in the fraction of proliferating T cells identified via CellTrace Violet staining. EBV-specific effector T cells' activities were measured with ELISA and Calcein release assays. For IFN-γ detection from T cells, effector and target cells were seeded at 5×10^4 cell per ml (1:1 ratio) each and co-cultured for 16 h in a 96-well plate (V bottom). IFN-γ levels were detected with ELISA. IFN-γ concentrations <16 pg/ml were considered as not detected.

T cell cytotoxicity assays

Primary infected B cells were purified by Ficoll-Hypaque gradient centrifugation, and 5×10^5 target cells were labeled with calcein at 0.5 µg/ml. After three washing steps with PBS, target and effector cells were co-cultured in a 96-well plate (V bottom) with different ratios in RPMI red phenol-free medium to reduce background signals. After 4 h of co-culture, fluorescence intensity of the released calcein was measured by the Infinite F200 PRO fluorometer (Tecan). As controls, spontaneous calcein release of target cells cultivated without effector cells and cells lysed with 0.5% Triton-X100 were used to define the levels of no and fully lysed target cells, respectively.

Statistical analysis

We used Prism 6.0 software (GraphPad) for the statistical analysis. A two-tailed ratio Student's *t* test was applied unless otherwise mentioned.

Online supplemental material

Fig. S1 shows the predicted miRNA-binding sites and mutations tested in 3′-UTR reporter assays. Table S1, available as an Excel file, lists the gene transcripts controlled by viral miRNAs. Table S2 lists the HLA allele information of donors used in co-culture experiments. Online supplemental material is available at http://www.jem.org/cgi/content/full/jem.20160248/DC1.

ACKNOWLEDGMENTS

We thank Christian Münz, Zurich, Elisabeth Kremmer, Anne-Wiebe Mohr, and Liridona Maliqi, Munich, for animal experiments, antibodies, T cell clones, and experimental assistance, respectively. We also thank Dagmar Pich for her experimental expertise and advice.

This work was financially supported by the Deutsche Forschungsgemeinschaft (SFB1054/TP B05 and TP A03, SFB1064/TP A13, and SFB-TR36/TP A04), Deutsche Krebshilfe (107277 and 109661), National Institutes of Health (RO1: CA70723 and PO1: CA022443), and personal grants of Deutscher Akademischer Austauschdienst to T. Tagawa (Studienstipendien für ausländische Graduierte aller wissenschaftlichen Fächer) and European Molecular Biology Organization to M. Bouvet.

The authors declare no competing financial interests.

Submitted: 18 February 2016
Accepted: 1 August 2016

Downloaded from on September 29, 2016

Published September 12, 2016

REFERENCES

Adhikary, D., U. Behrends, A. Moosmann, K. Witter, G.W. Bornkamm, and J. Mautner. 2006. Control of Epstein-Barr virus infection in vitro by T helper cells specific for virion glycoproteins. *J. Exp. Med.* 203:995–1006. http://dx.doi.org/10.1084/jem.20051287

Adhikary, D., U. Behrends, H. Boerschmann, A. Pfünder, S. Burdach, A. Moosmann, K. Witter, G.W. Bornkamm, and J. Mautner. 2007. Immunodominance of lytic cycle antigens in Epstein-Barr virus-specific $CD4^+$ T cell preparations for therapy. *PLoS One.* 2:e583. http://dx.doi.org/10.1371/journal.pone.0000583

Bartel, D.P. 2004. MicroRNAs: genomics, biogenesis, mechanism, and function. *Cell.* 116:281–297. http://dx.doi.org/10.1016/S0092-8674(04)00045-5

Bartel, D.P. 2009. MicroRNAs: target recognition and regulatory functions. *Cell.* 136:215–233. http://dx.doi.org/10.1016/j.cell.2009.01.002

Barth, S., G. Meister, and F.A. Grässer. 2011. EBV-encoded miRNAs. *Biochim. Biophys. Acta.* 1809:631–640. http://dx.doi.org/10.1016/j.bbagrm.2011.05.010

Blum, J.S., P.A. Wearsch, and P. Cresswell. 2013. Pathways of antigen processing. *Annu. Rev. Immunol.* 31:443–473. http://dx.doi.org/10.1146/annurev-immunol-032712-095910

Boss, I.W., and R. Renne. 2011.Viral miRNAs and immune evasion. *Biochim. Biophys. Acta.* 1809:708–714. http://dx.doi.org/10.1016/j.bbagrm.2011.06.012

Cai, X., A. Schäfer, S. Lu, J.P. Bilello, R.C. Desrosiers, R. Edwards, N. Raab-Traub, and B.R. Cullen. 2006. Epstein-Barr virus microRNAs are evolutionarily conserved and differentially expressed. *PLoS Pathog.* 2:e23. http://dx.doi.org/10.1371/journal.ppat.0020023

Curtsinger, J.M., and M.F. Mescher. 2010. Inflammatory cytokines as a third signal for T cell activation. *Curr. Opin. Immunol.* 22:333–340. http://dx.doi.org/10.1016/j.coi.2010.02.013

Dobin, A., C.A. Davis, F. Schlesinger, J. Drenkow, C. Zaleski, S. Jha, P. Batut, M. Chaisson, and T.R. Gingeras. 2013. STAR: ultrafast universal RNA-seq aligner. *Bioinformatics.* 29:15–21. http://dx.doi.org/10.1093/bioinformatics/bts635

Dölken, L., G. Malterer, F. Erhard, S. Kothe, C.C. Friedel, G. Suffert, L. Marcinowski, N. Motsch, S. Barth, M. Beitzinger, et al. 2010. Systematic analysis of viral and cellular microRNA targets in cells latently infected with human γ-herpesviruses by RISC immunoprecipitation assay. *Cell Host Microbe.* 7:324–334. http://dx.doi.org/10.1016/j.chom.2010.03.008

Erhard, F., L. Dölken, L. Jaskiewicz, and R. Zimmer. 2013. PARma: identification of microRNA target sites in AGO-PAR-CLIP data. *Genome Biol.* 14:R79. http://dx.doi.org/10.1186/gb-2013-14-7-r79

Feederle, R., J. Haar, K. Bernhardt, S.D. Linnstaedt, H. Bannert, H. Lips, B.R. Cullen, and H.-J. Delecluse. 2011a. The members of an Epstein-Barr virus microRNA cluster cooperate to transform B lymphocytes. *J. Virol.* 85:9801–9810. http://dx.doi.org/10.1128/JVI.05100-11

Feederle, R., S.D. Linnstaedt, H. Bannert, H. Lips, M. Bencun, B.R. Cullen, and H.-J. Delecluse. 2011b. A viral microRNA cluster strongly potentiates the transforming properties of a human herpesvirus. *PLoS Pathog.* 7:e1001294. http://dx.doi.org/10.1371/journal.ppat.1001294

Garcia, D.M., D. Baek, C. Shin, G.W. Bell, A. Grimson, and D.P. Bartel. 2011. Weak seed-pairing stability and high target-site abundance decrease the proficiency of lsy-6 and other microRNAs. *Nat. Struct. Mol. Biol.* 18:1139–1146. http://dx.doi.org/10.1038/nsmb.2115

Gottschalk, S., C.M. Rooney, and H.E. Heslop. 2005. Post-transplant lymphoproliferative disorders. *Annu. Rev. Med.* 56:29–44. http://dx.doi.org/10.1146/annurev.med.56.082103.104727

Gottwein, E., D.L. Corcoran, N. Mukherjee, R.L. Skalsky, M. Hafner, J.D. Nusbaum, P. Shamulailatpam, C.L. Love, S.S. Dave, T. Tuschl, et al. 2011. Viral microRNA targetome of KSHV-infected primary effusion lymphoma cell lines. *Cell Host Microbe.* 10:515–526. http://dx.doi.org/10.1016/j.chom.2011.09.012

Grundhoff, A., and C.S. Sullivan. 2011.Virus-encoded microRNAs. *Virology.* 411:325–343. http://dx.doi.org/10.1016/j.virol.2011.01.002

Haneklaus, M., M. Gerlic, M. Kurowska-Stolarska, A.-A. Rainey, D. Pich, I.B. McInnes, W. Hammerschmidt, L.A.J. O'Neill, and S.L. Masters. 2012. Cutting edge: miR-223 and EBV miR-BART15 regulate the NLRP3 inflammasome and IL-1β production. *J. Immunol.* 189:3795–3799. http://dx.doi.org/10.4049/jimmunol.1200312

Haque, T., G.M. Wilkie, M.M. Jones, C.D. Higgins, G. Urquhart, P. Wingate, D. Burns, K. McAulay, M. Turner, C. Bellamy, et al. 2007. Allogeneic cytotoxic T-cell therapy for EBV-positive posttransplantation lymphoproliferative disease: results of a phase 2 multicenter clinical trial. *Blood.* 110:1123–1131. http://dx.doi.org/10.1182/blood-2006-12-063008

Hislop, A.D., N.E. Annels, N.H. Gudgeon, A.M. Leese, and A.B. Rickinson. 2002. Epitope-specific evolution of human CD8(+) T cell responses from primary to persistent phases of Epstein-Barr virus infection. *J. Exp. Med.* 195:893–905. http://dx.doi.org/10.1084/jem.20011692

IARC Working Group on the Evaluation of Carcinogenic Risks to Humans. 2010. IARC monographs on the evaluation of carcinogenic risks to humans. Ingested nitrate and nitrite, and cyanobacterial peptide toxins. *IARC Monogr. Eval. Carcinog. Risks Hum.* 94:v–vii: 1–412.

Icheva, V., S. Kayser, D. Wolff, S. Tuve, C. Kyzirakos, W. Bethge, J. Greil, M.H. Albert, W. Schwinger, M. Nathrath, et al. 2013. Adoptive transfer of Epstein-Barr virus (EBV) nuclear antigen 1-specific T cells as treatment for EBV reactivation and lymphoproliferative disorders after allogeneic stem-cell transplantation. *J. Clin. Oncol.* 31:39–48. http://dx.doi.org/10.1200/JCO.2011.39.8495

Iskra, S., M. Kalla, H.J. Delecluse, W. Hammerschmidt, and A. Moosmann. 2010.Toll-like receptor agonists synergistically increase proliferation and activation of B cells by Epstein-Barr virus. *J. Virol.* 84:3612–3623. http://dx.doi.org/10.1128/JVI.01400-09

Iwakiri, D., L. Zhou, M. Samanta, M. Matsumoto, T. Ebihara, T. Seya, S. Imai, M. Fujieda, K. Kawa, and K. Takada. 2009. Epstein-Barr virus (EBV)-encoded small RNA is released from EBV-infected cells and activates signaling from Toll-like receptor 3. *J. Exp. Med.* 206:2091–2099. http://dx.doi.org/10.1084/jem.20081761

Jochum, S., A. Moosmann, S. Lang, W. Hammerschmidt, and R. Zeidler. 2012. The EBV immunoevasins vIL-10 and BNLF2a protect newly infected B cells from immune recognition and elimination. *PLoS Pathog.* 8:e1002704. http://dx.doi.org/10.1371/journal.ppat.1002704

Johannsen, E., M. Luftig, M.R. Chase, S. Weicksel, E. Cahir-McFarland, D. Illanes, D. Sarracino, and E. Kieff. 2004. Proteins of purified Epstein-Barr virus. *Proc. Natl. Acad. Sci. USA.* 101:16286–16291. http://dx.doi.org/10.1073/pnas.0407320101

Kalla, M., and W. Hammerschmidt. 2012. Human B cells on their route to latent infection--early but transient expression of lytic genes of Epstein-Barr virus. *Eur. J. Cell Biol.* 91:65–69. http://dx.doi.org/10.1016/j.ejcb.2011.01.014

Kalla, M., A. Schmeinck, M. Bergbauer, D. Pich, and W. Hammerschmidt. 2010. AP-1 homolog BZLF1 of Epstein-Barr virus has two essential functions dependent on the epigenetic state of the viral genome. *Proc. Natl. Acad. Sci. USA.* 107:850–855. http://dx.doi.org/10.1073/pnas.0911948107

Kieser, A., and K.R. Sterz. 2015. The Latent Membrane Protein 1 (LMP1). *Curr. Top. Microbiol. Immunol.* 391:119–149.

Klinke, O., R. Feederle, and H.-J. Delecluse. 2014. Genetics of Epstein-Barr virus microRNAs. *Semin. Cancer Biol.* 26:52–59. http://dx.doi.org/10.1016/j.semcancer.2014.02.002

Kuzembayeva, M., Y.-F. Chiu, and B. Sugden. 2012. Comparing proteomics and RISC immunoprecipitations to identify targets of Epstein-Barr

Downloaded from on September 29, 2016

Published September 12, 2016

viral miRNAs. *PLoS One.* 7:e47409. http://dx.doi.org/10.1371/journal.pone.0047409

Lo, A.K.F., K.F. To, K.W. Lo, R.W.-M. Lung, J.W.Y. Hui, G. Liao, and S.D. Hayward. 2007. Modulation of LMP1 protein expression by EBV-encoded microRNAs. *Proc. Natl. Acad. Sci. USA.* 104:16164–16169. http://dx.doi.org/10.1073/pnas.0702896104

Long, H.M., A.M. Leese, O.L. Chagoury, S.R. Connerty, J. Quarcoopome, L.L. Quinn, C. Shannon-Lowe, and A.B. Rickinson. 2011. Cytotoxic $CD4^+$ T cell responses to EBV contrast with CD8 responses in breadth of lytic cycle antigen choice and in lytic cycle recognition. *J. Immunol.* 187:92–101. http://dx.doi.org/10.4049/jimmunol.1100590

Milosevic, S., U. Behrends, H. Christoph, and J. Mautner. 2005. Direct mapping of MHC class II epitopes. *J. Immunol. Methods.* 306:28–39. http://dx.doi.org/10.1016/j.jim.2005.07.020

Moosmann, A., I. Bigalke, J. Tischer, L. Schirrmann, J. Kasten, S. Tippmer, M. Leeping, D. Prevalsek, G. Jaeger, G. Ledderose, et al. 2010. Effective and long-term control of EBV PTLD after transfer of peptide-selected T cells. *Blood.* 115:2960–2970. http://dx.doi.org/10.1182/blood-2009-08-236356

Nachmani, D., N. Stern-Ginossar, R. Sarid, and O. Mandelboim. 2009. Diverse herpesvirus microRNAs target the stress-induced immune ligand MICB to escape recognition by natural killer cells. *Cell Host Microbe.* 5:376–385. http://dx.doi.org/10.1016/j.chom.2009.03.003

Nimmerjahn, F., D. Kobelt, A. Steinkasserer, A. Menke, G. Hobom, U. Behrends, G.W. Bornkamm, and J. Mautner. 2003. Efficient generation and expansion of antigen-specific $CD4^+$ T cells by recombinant influenza viruses. *Eur. J. Immunol.* 33:3331–3341. http://dx.doi.org/10.1002/eji.200324342

Qiu, J., K. Cosmopoulos, M. Pegtel, E. Hopmans, P. Murray, J. Middeldorp, M. Shapiro, and D.A. Thorley-Lawson. 2011. A novel persistence associated EBV miRNA expression profile is disrupted in neoplasia. *PLoS Pathog.* 7:e1002193. http://dx.doi.org/10.1371/journal.ppat.1002193

Quinn, L.L., L.R. Williams, C. White, C. Forrest, J. Zuo, and M. Rowe. 2015. The missing link in Epstein-Barr virus immune evasion: the BDLF3 gene induces ubiquitination and downregulation of major histocompatibility complex class I (MHC-I) and MHC-II. *J. Virol.* 90:356–367. http://dx.doi.org/10.1128/JVI.02183-15

Rancan, C., L. Schirrmann, C. Hüls, R. Zeidler, and A. Moosmann. 2015. Latent membrane protein LMP2A impairs recognition of EBV-infected cells by $CD8^+$ T cells. *PLoS Pathog.* 11:e1004906. http://dx.doi.org/10.1371/journal.ppat.1004906

Rehmsmeier, M., P. Steffen, M. Höchsmann, and R. Giegerich. 2004. Fast and effective prediction of microRNA/target duplexes. *RNA.* 10:1507–1517. http://dx.doi.org/10.1261/rna.5248604

Ressing, M.E., D. van Leeuwen, F.A.W. Verreck, R. Gomez, B. Heemskerk, M. Toebes, M.M. Mullen, T.S. Jardetzky, R. Longnecker, M.W. Schilham, et al. 2003. Interference with T cell receptor-HLA-DR interactions by Epstein-Barr virus gp42 results in reduced T helper cell recognition. *Proc. Natl. Acad. Sci. USA.* 100:11583–11588. http://dx.doi.org/10.1073/pnas.2034960100

Ressing, M.E., D. Horst, B.D. Griffin, J. Tellam, J. Zuo, R. Khanna, M. Rowe, and E.J.H.J. Wiertz. 2008. Epstein-Barr virus evasion of $CD8^+$ and $CD4^+$ T cell immunity via concerted actions of multiple gene products. *Semin. Cancer Biol.* 18:397–408. http://dx.doi.org/10.1016/j.semcancer.2008.10.008

Ressing, M.E., M. van Gent, A.M. Gram, M.J.G. Hooykaas, S.J. Piersma, and E.J.H.J. Wiertz. 2015. Immune evasion by Epstein-Barr virus. *Curr. Top. Microbiol. Immunol.* 391:355–381. http://dx.doi.org/10.1007/978-3-319-22834-1_12

Riley, K.J., G.S. Rabinowitz, T.A. Yario, J.M. Luna, R.B. Darnell, and J.A. Steitz. 2012. EBV and human microRNAs co-target oncogenic and apoptotic viral and human genes during latency. *EMBO J.* 31:2207–2221. http://dx.doi.org/10.1038/emboj.2012.63

Rowe, M., B. Glaunsinger, D. van Leeuwen, J. Zuo, D. Sweetman, D. Ganem, J. Middeldorp, E.J.H.J. Wiertz, and M.E. Ressing. 2007. Host shutoff during productive Epstein-Barr virus infection is mediated by BGLF5 and may contribute to immune evasion. *Proc. Natl. Acad. Sci. USA.* 104:3366–3371. http://dx.doi.org/10.1073/pnas.0611128104

Samanta, M., D. Iwakiri, T. Kanda, T. Imaizumi, and K. Takada. 2006. EB virus-encoded RNAs are recognized by RIG-I and activate signaling to induce type I IFN. *EMBO J.* 25:4207–4214. http://dx.doi.org/10.1038/sj.emboj.7601314

Seto, E., A. Moosmann, S. Grömminger, N. Walz, A. Grundhoff, and W. Hammerschmidt. 2010. Micro RNAs of Epstein-Barr virus promote cell cycle progression and prevent apoptosis of primary human B cells. *PLoS Pathog.* 6:e1001063. http://dx.doi.org/10.1371/journal.ppat.1001063

Skalsky, R.L., and B.R. Cullen. 2010. Viruses, microRNAs, and host interactions. *Annu. Rev. Microbiol.* 64:123–141. http://dx.doi.org/10.1146/annurev.micro.112408.134243

Skalsky, R.L., D.L. Corcoran, E. Gottwein, C.L. Frank, D. Kang, M. Hafner, J.D. Nusbaum, R. Feederle, H.-J. Delecluse, M.A. Luftig, et al. 2012. The viral and cellular microRNA targetome in lymphoblastoid cell lines. *PLoS Pathog.* 8:e1002484. http://dx.doi.org/10.1371/journal.ppat.1002484

Steinbrück, L., M. Gustems, S. Medele, T.F. Schulz, D. Lutter, and W. Hammerschmidt. 2015. K1 and K15 of Kaposi's sarcoma-associated herpesvirus are partial functional homologues of latent membrane protein 2A of Epstein-Barr virus. *J. Virol.* 89:7248–7261. http://dx.doi.org/10.1128/JVI.00839-15

Szabo, S.J., B.M. Sullivan, S.L. Peng, and L.H. Glimcher. 2003. Molecular mechanisms regulating Th1 immune responses. *Annu. Rev. Immunol.* 21:713–758. http://dx.doi.org/10.1146/annurev.immunol.21.120601.140942

Thorley-Lawson, D.A. 2005. EBV the prototypical human tumor virus--just how bad is it? *J. Allergy Clin. Immunol.* 116:251–261. http://dx.doi.org/10.1016/j.jaci.2005.05.038

Vereide, D.T., E. Seto, Y.-F. Chiu, M. Hayes, T. Tagawa, A. Grundhoff, W. Hammerschmidt, and B. Sugden. 2014. Epstein-Barr virus maintains lymphomas via its miRNAs. *Oncogene.* 33:1258–1264. http://dx.doi.org/10.1038/onc.2013.71

Verhoeven, R.J.A., S. Tong, G. Zhang, J. Zong, Y. Chen, D.-Y. Jin, M.-R. Chen, J. Pan, and H. Chen. 2016. NF-κB signaling regulates expression of Epstein-Barr virus BART microRNAs and long noncoding RNAs in nasopharyngeal carcinoma. *J. Virol.* 00613–16. http://dx.doi.org/10.1128/JVI.00613-16

Wen, W., D. Iwakiri, K. Yamamoto, S. Maruo, T. Kanda, and K. Takada. 2007. Epstein-Barr virus BZLF1 gene, a switch from latency to lytic infection, is expressed as an immediate-early gene after primary infection of B lymphocytes. *J. Virol.* 81:1037–1042. http://dx.doi.org/10.1128/JVI.01416-06

Wiesner, M., C. Zentz, C. Mayr, R. Wimmer, W. Hammerschmidt, R. Zeidler, and A. Moosmann. 2008. Conditional immortalization of human B cells by CD40 ligation. *PLoS One.* 3:e1464. http://dx.doi.org/10.1371/journal.pone.0001464

Wu, Y., S. Maruo, M. Yajima, T. Kanda, and K. Takada. 2007. Epstein-Barr virus (EBV)-encoded RNA 2 (EBER2) but not EBER1 plays a critical role in EBV-induced B-cell growth transformation. *J. Virol.* 81:11236–11245. http://dx.doi.org/10.1128/JVI.00579-07

Xia, T., A. O'Hara, I. Araujo, J. Barreto, E. Carvalho, J.B. Sapucaia, J.C. Ramos, E. Luz, C. Pedroso, M. Manrique, et al. 2008. EBV microRNAs in primary lymphomas and targeting of CXCL-11 by ebv-mir-BHRF1-3. *Cancer Res.* 68:1436–1442. http://dx.doi.org/10.1158/0008-5472.CAN-07-5126

Downloaded from on September 29, 2016

Published September 12, 2016

Zuo, J., A. Currin, B.D. Griffin, C. Shannon-Lowe, W.A. Thomas, M.E. Ressing, E.J.H.J. Wiertz, and M. Rowe. 2009. The Epstein-Barr virus G-protein-coupled receptor contributes to immune evasion by targeting MHC class I molecules for degradation. *PLoS Pathog.* 5:e1000255. http://dx.doi.org/10.1371/journal.ppat.1000255

Zuo, J., W.A. Thomas, T.A. Haigh, L. Fitzsimmons, H.M. Long, A.D. Hislop, G.S. Taylor, and M. Rowe. 2011. Epstein-Barr virus evades $CD4^+$ T cell responses in lytic cycle through BZLF1-mediated downregulation of CD74 and the cooperation of vBcl-2. *PLoS Pathog.* 7:e1002455. http://dx.doi.org/10.1371/journal.ppat.1002455

Downloaded from on September 29, 2016